Structural Characterization of Epitaxial LSMO Thin Films Grown on LSAT Substrates

M. Španková[a,*], E. Dobročka[a], V. Štrbík[a], Š. Chromik[a], N. Gál[a], N. Nedelko[b], A. Ślawska-Waniewska[b] and P. Gierłowski[b]

[a]Institute of Electrical Engineering, Slovak Academy of Sciences, Dúbravská cesta 9, 841 04 Bratislava, Slovakia
[b]Institute of Physics, Polish Academy of Sciences, Aleja Lotnikow 32/46, PL-02668 Warsaw, Poland

High resolution X-ray measurements were used to characterize the crystalline structure of $La_{0.67}Sr_{0.33}MnO_3$ (LSMO) thin films grown on $La_{0.26}Sr_{0.76}Al_{0.61}Ta_{0.37}O_3$ (LSAT) substrate under a small compressive strain (-0.2%). The accommodation of lattice mismatch gives rise to a lattice modulation in the structure. A series of linear h scans (rocking curves) across LSMO 004 diffraction for various values of ϕ angle (rotation of sample around [001] axis) was performed to provide better insight into this structural feature. Despite the cubic structure of the substrate the stress relief mechanism of the LSMO film is considerably anisotropic. Whereas in [010] substrate direction no LSMO lattice modulation was observed, in [100] direction a lattice modulation was developed having no influence on good electrical properties of the prepared LSMO films.

1. Introduction

Perovskite manganite LSMO has been one of the most extensively studied colossal magnetoresistance (CMR) material because of its high Curie temperature (T_C), the temperature at which the CMR materials undergo a ferromagnetic–paramagnetic transition and simultaneously metal–insulator transition at T_{MI} according to double exchange theory. Hence, the LSMO thin films reveal a great potential for industrial applications. On the other hand, the substrates underneath the LSMO films can significantly influence the structural, electrical, and magnetic properties of the LSMO films due to a lattice-mismatch-induced biaxial strain. Millis et al. [1] reported that the T_C of manganites is strongly sensitive to biaxial strain and a 1% biaxial strain would cause a 10% shift in T_C. The decrease of the T_C (T_{MI}) with increasing strain was experimentally observed [2, 3]. Therefore, it takes a great effort to use a substrate with the best lattice matching to the LSMO. The bulk manganite LSMO can be described as a slightly deformed pseudocubic perovskite lattice with a lattice parameter $a_{bulk} = 0.3876$ nm and a unit cell angle $90.26°$. The unit cell of the LSAT substrate can also be characterized as a pseudocubic one with $a = 0.3868$ nm. The nominal lattice mismatch between the bulk LSMO and the LSAT substrate is very small (-0.2%), so the LSMO films are subjected to a very little compressive strain. For comparison, other frequently used substrates exhibit the following lattice mismatch to the LSMO: $SrTiO_3$ (001) $+0.75\%$, $LaAlO_3$ (001) -2.14%, MgO (001) $+8.1\%$, $NdGaO_3$(110) -0.6%.

Despite some growth peculiarities, like long-range lattice modulation [4, 5], superlattice formation [6] or structural domains with angular-distortion strain [7] the LSMO films grown on the LSAT exhibit high T_C (T_{MI}) values ≈ 360 K [4, 8] and resistivity < 100 $\mu\Omega$ cm at low temperatures [2, 8]. All these growth peculiarities can be detected in rocking curves as additional satellite peaks (even in multiple form) on both sides of a central diffraction peak and as a broad diffuse scattering peak below the central peak.

In this contribution we investigate microstructural properties of epitaxial LSMO films (with high T_C of 360 K) using high resolution X-ray diffraction (θ–2θ scans, φ-scans, linear h and l scans in reciprocal space).

2. Experimental details

The LSMO films were deposited onto a one-side polished (001) oriented single crystalline LSAT substrates using pulsed laser deposition (PLD) system. The depositions conditions of LSMO were described elsewhere [7]. The thickness of the LSMO films varied between 20 and 47 nm. A Bruker D8 DISCOVER diffractometer equipped with with rotating Cu anode operating at 12 kW was used to determine the crystallographic orientation perpendicular to the film surface (θ–2θ configuration). To determine the in-plane orientation of the LSMO films with respect to the major axes of the substrates, φ-scans were carried out. Linear h and l scans in the reciprocal space were performed in high-resolution setup with Bartels monochromator in the primary beam to determine lattice parameters, as well as the fine structure of the LSMO films. The surface morphology was investigated with a commercial atomic force microscopy (AFM). Magnetic measurements were performed by means of

---

*corresponding author; e-mail: marianna.spankova@savba.sk

a commercial PPMS-9T system equipped with a vibrating sample magnetometer (VSM) and a VSM electromagnet system equipped with a furnace. The temperature dependences of dc magnetization were measured at decreasing temperature in range from 400 K to 250 K, keeping all the time the same external magnetic field ($B = 5$ mT). The magnetic field dependences of the in-plane magnetization were recorded in the field range ± 0.3 T at selected temperatures. For the resistivity vs. temperature $\rho(T)$ dependences a standard four-point probe method was applied.

3. Results and discussions

All prepared LSMO films exhibited very good crystalline quality. AFM reveals the growth of surface irregularities with lateral dimensions of 30–50 nm. The root-mean-square of the roughness values for a 20 nm and 47 nm thick LSMO films are about 0.8 nm and 1.2 nm, respectively. In the θ–2θ scan only LSMO $00l$ diffractions were present, indicating the absence of any spurious phase. To determine the in-plane growth properties, φ-scans of the LSMO 204 and substrate 204 diffractions were carried out. We observed four sharp maxima indicating the fourfold symmetry of the LSMO lattice. The in-plane $a_{\parallel}$ and out-of plane $a_{\perp}$ lattice parameters of the LSMO film (thickness 20 nm) estimated from h and l linear scans are 0.3868 nm and 0.3889 nm, respectively. The strains in the LSMO films are expressed as $\varepsilon_{\parallel} = (a_{\parallel} - a_{\text{bulk}})/a_{\text{bulk}}$ for in-plane strain and $\varepsilon_{\perp} = (a_{\perp} - a_{\text{bulk}})/a_{\text{bulk}}$ for out-of plane strain. The values of $\varepsilon_{\parallel} = -0.2\%$ and $\varepsilon_{\perp} = 0.34\%$ confirmed that LSMO films on LSAT exhibit only small strains. To determine the crystallinity of these films h scans (rocking curves, RCs) across the $00l$ diffractions of the LSMO were performed. The RCs for directions corresponding to [100] and [010] axes of the substrate (curve 1, curve 2, respectively), shown in Fig. 1, indicate that the LSMO crystallizes in a different way. Curve 3 represents the RC of the LSAT substrate without LSMO but measured across the position of the LSMO peak, showing no contribution from the substrate to the LSMO film diffractions. The full width at half maximum (FWHM) of the RC (curve 2 in Fig. 1) reaches the value of about 0.07°. This value correlates well with the FWHM values of about 0.07° presented by other authors [8, 9].

In addition to the central maximum, two satellite peaks were recorded in the RC. Similar satellite maxima were reported by [5] in RCs of LSMO/LSAT epitaxial system. The authors ascribed the observed maxima to the presence of slight modulation of the layer lattice. They developed a simple kinematical model describing the lattice modulation and were able to simulate the shape of RCs using a few fitting parameters like modulation amplitude and periodicity. It has to be pointed out that the presence of the central peak indicates the long range coherence of the layer lattice, i.e. the layer is not divided into a slightly misoriented mosaic blocks. The mosaic
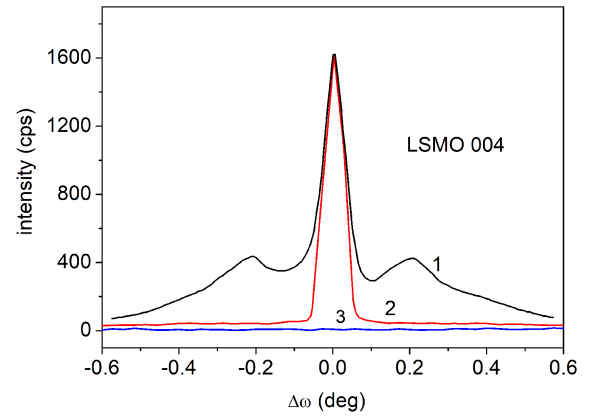
Fig. 1. Rocking curves taken from the 004 diffraction of the LSMO for [100] (curve 1) and [010] (curve 2) directions. Curve 3 is the rocking curve of the LSAT substrate (without LSMO). Curves 1 and 2 are shifted in vertical axis for better visibility.
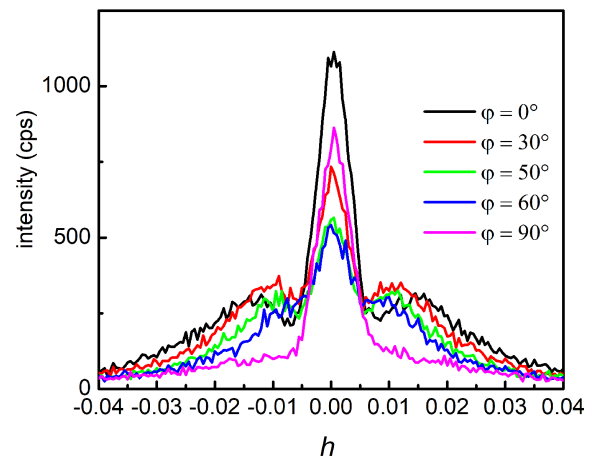
Fig. 2. Series of h scans across the 004 diffraction of the LSMO taken at various values of substrate rotation angle ϕ.

structure takes place in the systems with large lattice mismatch as e.g. LSMO/MgO [10]. Another important feature distinguishing between these two cases is the distance of the satellite peaks. In the case of layers with mosaic microstructure the distance of two maxima of RC expressed in h coordinate increases with the order of $00l$ diffractions preserving their angular distance. By contrast, the distance (in h coordinate) of satellite peaks resulting from the lattice modulation does not change with the order of diffractions as is the case of our samples. Interestingly, the modulation takes place only in one direction $\langle 100 \rangle$ of the substrate. The satellite maxima can be represented in reciprocal space as two diffraction spots beside the central spot (see Fig. 9 in Ref. [5]).

In order to specify the precise direction of the LSMO lattice modulation, a series of linear h scans across the layer diffraction spot 004 were recorded for various angles of sample rotation around the surface normal (Fig. 2).
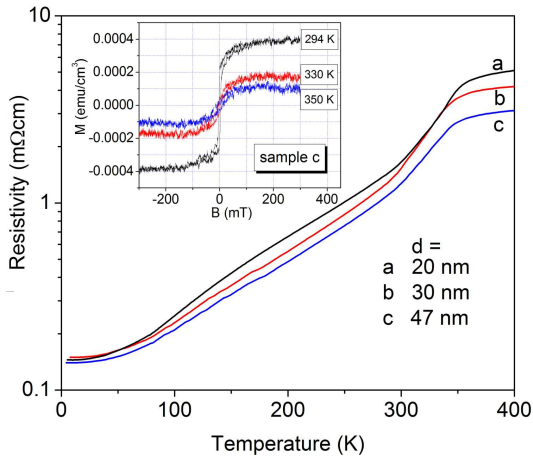
Fig. 3. $\rho(T)$ dependences for LSMO thin films grown on LSAT substrate. Inset shows the dependence of magnetization on applied magnetic field for film thickness of 47 nm.

The values $\varphi = 0°$ and $\varphi = 90°$ correspond to substrate directions [100] and [010], respectively. The distance of satellites is the largest for $\varphi = 0°$ and they overlap with the central peak for $\varphi = 90°$. Obviously, during the rotation of the sample around the normal by angle φ the satellite spots revolve around the central diffraction spot. Nevertheless, they can be detected although they do not lie precisely within the diffraction plane. This is a consequence of a certain insensitivity of the diffraction conditions to the sample tilting χ. Apparently, this movement is accompanied by decreasing distance of the corresponding satellite maxima in RC. On the basis of the outlined model it can be therefore concluded that the lattice modulation really occurs in the substrate direction [100]. The decreasing intensities of h scans for increasing angle φ in Fig. 2 are caused by irregular shape of the sample. The sample dimension in [010] direction is about twice the dimension in [100] direction. Therefore the irradiated and diffracting volume changes decreased with increasing angle φ.

Typical temperature dependences of resistivity ($\rho(T)$) of the LSMO films of various thicknesses are shown in Fig. 3. A low temperature residual resistivity ρ_0 reaches values of 150 $\mu\Omega$ cm, approximately 2–3 times higher than presented in [2]. The domain structure and boundaries between the domains can contribute to the increased values of ρ_0. The resistivity at room temperature is about 1 mΩ cm. Maximal resistivity changes were observed at the temperature around 335 K. The observed lattice modulation has no influence on the electrical properties of our LSMO films, we did not register any angular dependence of the resistivity.

4. Conclusions

We prepared LSMO thin films by PLD on LSAT substrate. Due to a small lattice mismatch between the LSMO and the substrate (-0.2%) the LSMO films are subjected to very little compressive strain. θ–2θ scans and φ-scans confirmed epitaxial growth of the LSMO films. We registered satellite peaks in the h scans indicating the presence of lattice modulation. The lattice modulation is developing to relieve stress due to the mismatch strain between LSMO and the underlying substrate. Mapping of stress relief we detected a modulation of the LSMO lattice in [100] substrate direction. In spite of structural peculiarities the LSMO films exhibit very good electrical properties as well as high Curie temperature of 360 K.

References

[1]   A.J. Millis, T. Darling, A. Migliori, *J. Appl. Phys.* **83**, 1588 (1998).

[2]   Y. Takamura, R.V. Chopdekar, E. Arenholz, Y. Suzuki, *Appl. Phys. Lett.* **92**, 162504-3 (2008).

[3]   Y. Lu, J. Klein, F. Herbstritt, J.B. Philipp, A. Marx, R. Gross, *Phys. Rev. B* **73**, 184406-7 (2006).

[4]   H. Boschker, M. Mathews, P. Brinks, E. Houwmana, A. Vailionis, G. Koster, D.H.A. Blank, G. Rijnders, *J. Magn. Magn. Mater.* **323**, 2632 (2011).

[5]   A. Vailionis, H. Boschker, W. Siemons, E.P. Houwman, D.H.A. Blank, G. Rijnders, G. Koster, *Phys. Rev. B* **83**, 064101 (2011).

[6]   T.F. Zhou, G. Li, X.G. Li, S.W. Jin, W.B. Wu, *Appl. Phys. Lett.* **90**, 042512-3 (2007).

[7]   M. Španková, V. Štrbík, E. Dobročka, Š. Chromik, M. Sojková, D.N. Zheng, J. Li, *Vacuum* **126**, 24 (2016).

[8]   S. Jin, G. Gao, W. Wu, X. Zhou, *J. Phys. D* **40**, 305 (2007).

[9]   Yu.A. Boikov, T. Claeson, V.A. Danilov, *Phys. Solid State* **47**, 2281 (2005).

[10] M. Španková, A. Rosová, E. Dobročka, Š. Chromik, I. Vávra, V. Štrbík, D. Machajdík, A.P. Kobzev, M. Sojková, *Thin Solid Films* **583**, 19 (2015).